Robust approach to maximize the range and accuracy of force application in atomic force microscopes with nonlinear position-sensitive detectors

E C C M Silva and K J Van Vliet

Department of Materials Science and Engineering, Massachusetts Institute of Technology, Cambridge, MA 02139, USA

E-mail: krystyn@mit.edu (K J Van Vliet)

Abstract
The atomic force microscope is used increasingly to investigate the mechanical properties of materials via sample displacement under an applied force. However, both the extent of forces attainable and the accuracy of those forces measurements are significantly limited by the optical lever configuration that is commonly used to infer nanoscale deflection of the cantilever. We present a robust and general approach to characterize and compensate for the nonlinearity of the position-sensitive optical device via data processing, requiring no modification of existing instrumentation. We demonstrate that application of this approach reduced the maximum systematic error on the gradient of a force–displacement response from 50% to 5%, and doubled the calibrated force application range. Finally, we outline an experimental protocol that optimizes the use of the quasi-linear range of the most commonly available optical feedback configurations and also accounts for the residual systematic error, allowing the user to benefit from the full detection range of these indirect force sensors.

1. Introduction

The atomic force microscope (AFM) [1] has become an important tool for investigating the mechanical properties of materials at the nanoscale via the analysis of force–displacement responses [2, 3]. In the most common experimental approach (figure 1), the deflection of the cantilever is measured using the optical lever technique [4]: a laser beam is reflected by the bent cantilever into a position-sensitive detector (PSD). The usual PSD is a split or quadrant photodiode, which records the difference between the light intensities received by the top section (A) and the bottom section (B) and converts this signal to a voltage output V_{PD}. The signal $V_{PD} = A - B$, usually normalized to the total intensity $A + B$, is a function of the beam position. This scheme is very sensitive to small changes in beam incident angle, detecting cantilever deflections of 0.1 Å or less, and measurement precision is usually limited by the thermal noise.
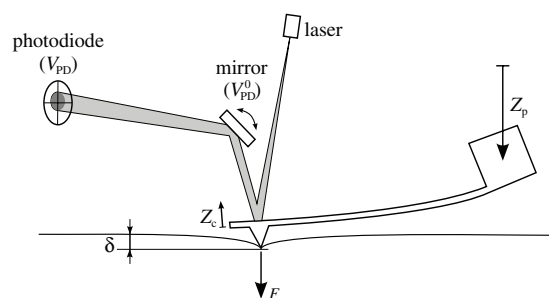
Figure 1. AFM force application configuration. A vertical displacement Z_p is applied to the cantilever base, causing it to deflect by Z_c and to apply a force F to the sample, which deforms by a depth δ. The deflection Z_c is measured indirectly through the photodiode, giving the deflection as a voltage signal V_{PD}. A mirror is used to adjust the resting signal V_{PD}^0 when $Z_c = 0$.

Unfortunately, the linear range of this laser-PSD configuration that is typically utilized in commercial AFMs is

limited, reducing the useful range of the PSD signal[1]. This limits the range of picoNewton- to microNewton scale forces accessible to the experimentalist, especially when compliant cantilevers (i.e. a spring constant less than 0.1 N m^{-1}) are used. Most of this nonlinearity is due to the shape of the laser spot [5], with small contributions (systematic error) from the geometry of the optical path [6]. While commercial AFM instrumentation is usually tuned to maximize the linear range, further extension of this range can be obtained by replacing the split photodiode with a linear PSD [7, 8] or an array detector [9].

Here, we demonstrate a method that determines and compensates for the nonlinearity of an existing PSD, and provide a protocol that allows the use of the full detection range of existing instrumentation based on a quadrant photodiode. This approach obviates the need for hardware replacements such as linear PSDs in order to take advantage of the full nominal range of forces that can be applied and measured accurately. In the following sections, we briefly review the usual calibration procedure and present a novel correction for this nonlinearity. Finally, we propose a protocol for the optimal use of an AFM for force–displacement acquisition.

2. Force–displacement measurement and traditional calibration

A simplified representation of the AFM force–displacement acquisition is shown in figure 1. The cantilever base displacement Z_p is controlled by the Z-piezoactuator, which displaces the probe toward the sample surface. When contact is made and the Z-piezo continues to travel toward the sample surface, the cantilever's free end deflects by Z_c. This bending mode of the cantilever deflects a laser beam focused near the free end, causing a differential voltage signal (termed the raw deflection V_{PD}) between the upper and lower segments of the quadrant photodiode into which this reflected laser beam is directed. This deflection of the cantilever also exerts a force F on the sample surface, calculated as:

$$F = k_c Z_c \tag{1}$$

where k_c is the cantilever spring constant. This force displaces the sample surface by a distance δ. When the probe tip is in contact with the sample, this deformation must be equal to the difference between the cantilever base displacement after contact $Z_p - Z_p^0$ and the cantilever free-end deflection Z_c:

$$\delta = Z_p - Z_p^0 - Z_c \tag{2}$$

where Z_p^0 is the base displacement at the contact point.

In such a force–displacement experiment, the only quantities that are measured directly are the vertical displacement of the Z-piezoactuator Z_p, acquired for example via a calibrated linear variable differential transformer (LVDT) in tandem, and the deflection angle of the cantilever probe,

acquired indirectly as the differential voltage V_{PD} in the photodiode.

In order to obtain a force–displacement (F, δ) response from the experimentally measured quantities, an accurate calibration of the relationship between the cantilever free-end deflection Z_c and the photodiode voltage V_{PD} is required.

Assuming that this relationship is linear, we can define a sensitivity S_{PD} as the slope of the V_{PD} versus Z_c curve. Thus, the voltage output is proportional to the cantilever deflection, and the signal V_{PD} (in (V)) corresponds directly to the cantilever deflection Z_c:

$$Z_c = (V_{PD} - V_{PD}^0)S_{PD}^{-1} \tag{3}$$

where the constant S_{PD}^{-1} is the inverse optical lever sensitivity (in (m V^{-1})) and V_{PD}^0 is the resting signal, or the photodiode voltage when the cantilever is not in contact with the sample surface. V_{PD}^0 can be adjusted manually to any desired value within the sensor range (typically to 0 V) by adjusting the mirror that deflects the laser beam toward the photodiode (see figure 1). From (1) to (3), it is clear that one can trivially obtain the force–displacement response $(F = k_c Z_c, \delta)$ from the experimental quantities Z_p and V_{PD}, if both S_{PD}^{-1} and k_c are known.

The inverse sensitivity S_{PD}^{-1} is obtained by performing an uncalibrated force–displacement test where the sample surface is much stiffer than the cantilever, such that the sample deflection δ is negligible and the cantilever free-end upward deflection Z_c is equal in magnitude to the Z-piezo downward displacement Z_p from the contact point Z_p^0:

$$\delta \approx 0 \longrightarrow Z_c = Z_p - Z_p^0. \tag{4}$$
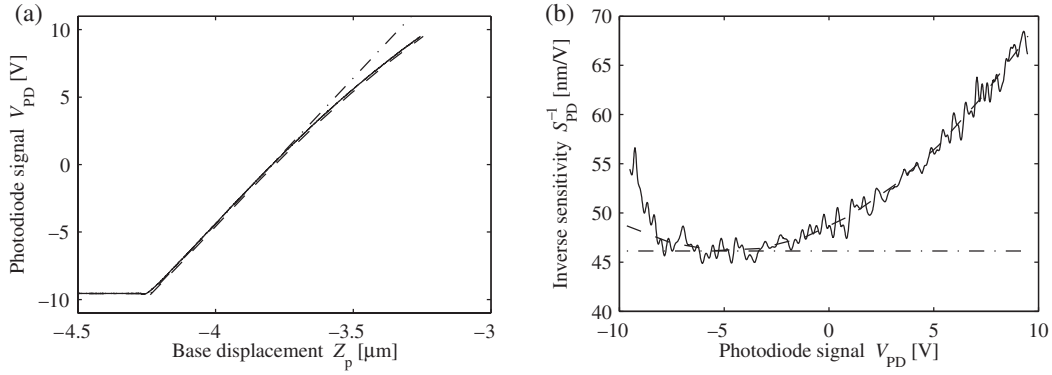
Comparing (3) and (4), we obtain the inverse sensitivity as the slope of the calibration curve, shown in figure 2 as the expected linear curve:

$$S_{PD}^{-1} = \frac{Z_p - Z_p^0}{V_{PD} - V_{PD}^0} = \frac{\Delta Z_p}{\Delta V_{PD}}. \tag{5}$$

3. Nonlinear calibration of the sensitivity

Actual force–displacement responses acquired to calibrate the inverse sensitivity S_{PD}^{-1} deviate from the ideal case described above, as shown in figure 2. Notably, the photodiode voltage V_{PD} versus Z-piezo displacement Z_p response, and thus the cantilever deflection Z_c versus V_{PD} relation, is nonlinear. The assumption that the inverse sensitivity S_{PD}^{-1} is a constant leads to increasing errors in the calculation of Z_c if V_{PD} is outside the linear range. In fact, figure 2 indicates up to 50% variation in S_{PD}^{-1} as a function of the range and initial value of the photodiode voltage for the cantilever considered (nominal spring constant $k_c = 42$ N m^{-1} [10]).

Among the several factors that introduce nonlinearities, the most important is the shape and intensity profile of the laser spot [3], as illustrated by figure 3. The sensitivity is proportional to the amount of light over the split line. If the spot is at the centre of the split photodiode, or nearly centred, the response is almost linear. As the spot moves away from the centre, nonlinearity becomes more pronounced due to the

---

[1] For the sensor analysed in section 4, the sensitivity is within 5% of the minimum value for a photodiode signal range of 7.5 V, which represents 38% of the total range of 20 V. For the specific cantilever employed, the measurements are reliable up to a load of 14.5 μN in ideal conditions, rather than the nominal maximum of 38.8 μN.

Figure 2. (a) Force calibration curve (V_{PD} versus Z) showing the expected linear response (— · —), the observed behaviour (solid line) and the proposed fit (– – –, offset for clarity). The rest signal is $V_{PD}^0 = -9.5$ V, as seen in the approach region. (b) The same curves expressed as S_{PD}^{-1} versus V_{PD}, obtained by calculating the slope dZ_p/dV_{PD} of the corresponding response in (a). The experimental response was smoothed before calculating the slope S_{PD}^{-1} using a finite difference formula. $V_{PD}^* = -4.8$ V is the minimum of this curve, and variation in S_{PD}^{-1} is minimized about this photodiode voltage.
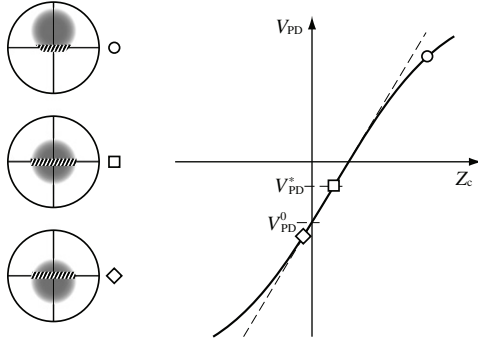
Figure 3. Effect of the laser spot shape on the response of a split photodiode. The area of the spot over the split line (hatched on the left figure) is proportional to the slope S_{PD}^{-1} of the optical sensitivity curve (V_{PD} versus Z_c, right). If the spot is centred (□) or nearly centred (◇), the response is almost linear. As the spot moves away from the centre (○), nonlinearity becomes more pronounced. The inflection point V_{PD}^* (□) and the resting signal V_{PD}^0 are marked in the graph.

faster change in the cross section and to the exponential decay of the light intensity.

If the spot shape is symmetric, the nonlinear response will be approximated well by a third-degree polynomial on V_{PD}, centred at the inflection point V_{PD}^* (see figure 3). The error is of the order $O(\Delta^5)$, where $\Delta = V_{PD} - V_{PD}^*$. If the shape is not symmetric, the error will be of the order $O(\Delta^4)$. We chose to fit a third-order polynomial to the (Z_c, V_{PD}) response of such loading calibration experiments:

$$Z_c = Z_p - Z_p^0 = a_3(V_{PD} - V_{PD}^*)^3 + a_1(V_{PD} - V_{PD}^*) + a_0 \quad (6)$$

where a_i are fitting parameters. In our experience, this produces an excellent fit to the experimental response of cantilever deflection against a rigid surface, which is not improved by additional terms $a_{i>3}$.

If required, the inverse sensitivity can be obtained as the derivative of this polynomial fit, a parabolic function of V_{PD}:

$$S_{PD}^{-1} = \frac{dZ_p}{dV_{PD}} = 3a_3(V_{PD} - V_{PD}^*)^2 + a_1. \quad (7)$$

Thus, the inverse sensitivity S_{PD}^{-1} is represented as a continuous function of the photodiode voltage V_{PD}, rather than as a single value. If the photodiode response were linear with V_{PD}, this function would be a horizontal line and there would be a single, constant S_{PD}^{-1} independent of V_{PD}.

4. Experimental verification

The experiments were carried out using a 3D-Molecular Force Probe (MFP-3D, from Asylum Research, Santa Barbara, CA). We used a silicon cantilever (Olympus AC160 [10]) of nominal spring constant $k_c = 42$ N m^{-1}. We performed several calibration experiments (deflection against a flat silicon surface), each time manually adjusting the resting photodiode voltage V_{PD}^0 to a series of values from -9.5 to 9.0 V in increments of 0.5 V. This calibration series was obtained in order to distinguish the effect of the inflection point V_{PD}^*, hypothesized to be a property solely of the photodiode, from other nonlinearities in the system (e.g. in the value of the Z-piezo displacement Z_p reported by the displacement transducer).

Figure 4 shows the resulting variation of the inverse sensitivity S_{PD}^{-1} as a function of the photodiode voltage V_{PD} for a subset of the curves acquired over a range of resting voltages V_{PD}^0. This figure illustrates that the S_{PD}^{-1} depends strongly on the absolute voltage V_{PD}. We note that the value of the inflection point V_{PD}^* varies depending on the resting voltage V_{PD}^0, suggesting that the quantities are not totally independent. However, $V_{PD}^* = -4.4$ V represents the approximate photodiode voltage at which the minimum S_{PD}^{-1} is obtained for this photodiode and this cantilever.

In order to further isolate the effect of the photodiode signal from any nonlinearities induced by the actual cantilever bending deflection upon contact with the rigid surface (Z_c, represented by $V_{PD} - V_{PD}^0$), we evaluated the inverse sensitivity S_{PD}^{-1} exactly at the contact point of the acquired loading response (i.e. in the absence of cantilever bending). Specifically, to each acquired V_{PD} versus Z_p response, equation (6) was fitted to determine the fitting constants a_i and the inflection point V_{PD}^*, and then equation (7) was evaluated
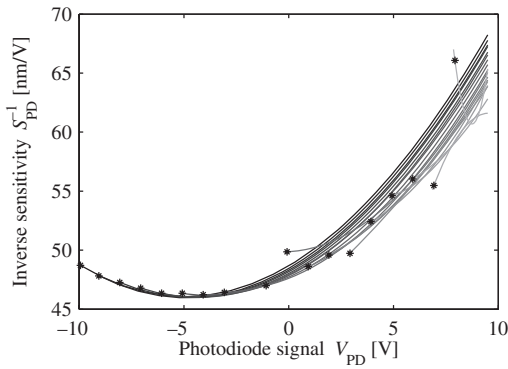
Figure 4. Inverse sensitivity S_{PD}^{-1} calculated via (7) as a function of the photodiode voltage V_{PD}. The resting point for each acquired response (V_{PD}^0) is marked with an asterisk. This demonstrates that most (but not all) of the nonlinearity in S_{PD}^{-1} is due to the photodiode nonlinearity. The remaining systematic error is indicated by the spread of values at any given V_{PD}.
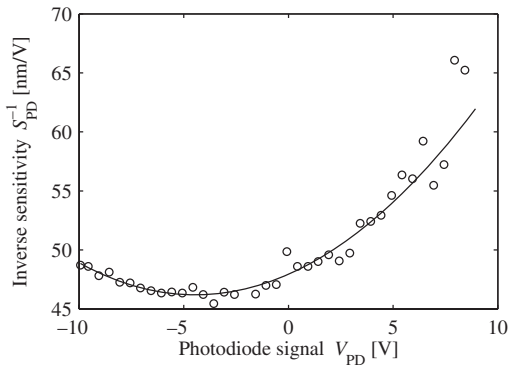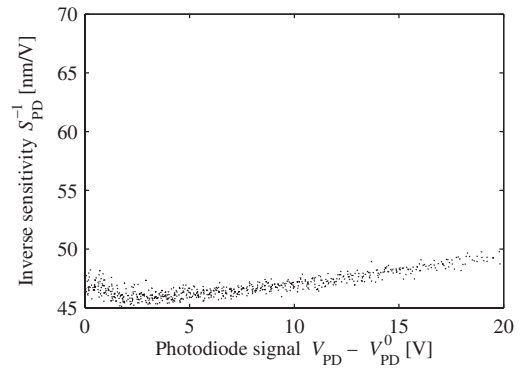

Figure 5. Inverse sensitivity $S_{PD}^{-1}(V_{PD}^0)$ evaluated at the contact point, as a function of the deflection $V_{PD} = V_{PD}^0$, and the corresponding global fit. Each experimental point represents a deflection response acquired at a different resting voltage V_{PD}^0; asterisks in figure 4 are in fact a subset of the larger set of experiments shown in this figure.

for the resting point $V_{PD} = V_{PD}^0$. Fitting a parabola to these points, we obtained an overall nonlinear behaviour that can be attributed solely to the nonlinearity of the photodiode output, as shown in figure 5.

We must note that an additional factor must be considered near the contact point. Since the cantilevered probe tip is sharp (with a nominal radius of $R = 7$ nm [10]), there is a small region of the force–displacement where the sample is indented and the approximation that sample deflection $\delta \approx 0$ is not valid. Nevertheless, fitting to the rest of the curve and extrapolating the gradient of this fit to $V_{PD} = V_{PD}^0$ gives the correct slope in the absence of physical indentation of the sample surface, whereas using the experimental slope at $V_{PD} = V_{PD}^0$ would introduce a significant error. This effect can be seen in figure 2(b), for $V_{PD} < -8$ V.

Using this global parabolic function $S_{PD}^{-1}(V_{PD})$, we recalculated the cantilever deflection Z_c from all acquired loading responses. That is, constants a_3, a_1 and V_{PD}^* were determined by fitting this parabolic function against (7), then Z_c was calculated from (6) (rather than from (3), which assumes a single value of the S_{PD}^{-1}). This approach

Figure 6. Apparent inverse sensitivity S_{PD}^{-1}, after correcting for the nonlinearity using the fit shown in figure 5 and smoothing to reduce the experimental noise. Data correspond to the uncorrected lines displayed in figure 4. The residual or systematic error is related to the physical deflection ($V_{PD} - V_{PD}^0$), rather than the absolute position V_{PD} of the laser spot on the photodiode.

compensated for all of the nonlinearity in the photodiode output, and the remaining systematic error resulted in a variation of about 5% in the slope of the calibration curve (Z_p versus Z_c), versus up to 50% before the compensation. This residual error is plotted in figure 6, as a function of the physical deflection signal ($V_{PD} - V_{PD}^0$). For easier comparison with the preceding figures, the slope dZ_p/dZ_c was multiplied by the inverse sensitivity $S_{PD}^{-1}(V_{PD}^*)$, giving an apparent inverse sensitivity. Upon correction of the PSD nonlinearity in this manner, the maximum calibrated force range increased from 14.5 μN (-8.15 to $+0.65$ V) to 38.8 μN (-10 to 10 V).

5. Proposed calibration protocol

Based on this study, we propose a calibration protocol that (a) identifies the linear range of the PSD and (b) corrects for the nonlinearity when processing the data. Working within the linear range identified in (a) allows the user to employ the linear assumption and neglect the nonlinear processing if the results are considered adequate.

Protocol:

 (i) Set the resting photodiode signal V_{PD}^0 near the lower range (e.g. -9.5 V if the range is -10 to 10 V) by adjusting the mirror position.

 (ii) Obtain an uncalibrated force–displacement response on a rigid substrate (calibration experiment) that approaches the upper range of the PSD output (e.g. to 9.5 V, to avoid saturation of the photodiode).

 (iii) Fit a third-order polynomial to the cantilever deflection $Z_c(V_{PD})$ response (6), and obtain the inflection point V_{PD}^*.

 (iv) Calculate the inverse sensitivity $S_{PD}^{-1}(V_{PD}^*)$ of the linear range using (7).

 (v) If the calibration of the cantilever spring constant k_c depends on the optical sensitivity (for example, if the Hutter and Bechhoefer method [11–13] is used), set the resting signal to $V_{PD}^0 = V_{PD}^*$ and obtain the cantilever spring constant at this point.

(vi) Calculate an optimal work range (minimum to maximum V_{PD}, centred in V_{PD}^*), according to the maximum force desired and the nominal stiffness of the cantilever. For example, if the goal is to apply 500 nN, S_{PD}^{-1} is 50 nm V^{-1} and $k_c = 1$ N m^{-1}, the V_{PD} range should be:

$$\frac{500 \text{ nN}}{1 \text{ N m}^{-1}} \times \frac{1}{50 \text{ nm V}^{-1}} = 10 \text{ V}$$

and, taking $V_{PD}^* = -4.5$ V, the optimal working range is -9.5 V to $+0.5$ V.

(vii) Optionally recalibrate (steps (i) to (iv)) within the working range, to compensate for the systematic error shown in figure 6.

(viii) Acquire the experimental V_{PD} versus Z_p response.

(ix) Calculate the cantilever deflection, by using either:

    (a) the conventional formula $Z_c = (V_{PD} - V_{PD}^0)S_{PD}^{-1}$, where S_{PD}^{-1} was obtained in step (iv); or

    (b) the nonlinear calibration curve $Z_c(V_{PD})$ obtained in step (iii) or (vii).

(x) Calculate the force using (1) and the sample displacement using (2).

6. Conclusions

It is well-known that the split photodiode position-sensitive device is intrinsically nonlinear except for very small deflections. While commercial AFM instrumentation is usually optimized such that the linear region is well centred and covers most of the sensor range, such nonlinearity still poses problems and limitations for applications where large forces (nanoNewton to microNewton scale) and/or very compliant ($k_c < 0.1$ N m^{-1}) cantilevers are employed.

The nonlinear calibration procedure presented here allows AFM users to benefit from the full range of their photodiode sensors without hardware modifications such as truly linear PSDs and photodiode arrays. It also improves the determination of the cantilever spring constant k_c for calibration methods that depend inherently on the optical lever sensitivity S_{PD}. This is the case for the Hutter and Bechhoefer method [11–13], which requires an accurate estimation of the thermal noise amplitude.

An analogous procedure can be employed to calibrate the lateral sensitivity of the PSD in conjunction with a lateral calibration method (e.g. [14, 15]). We expect that the strongly nonlinear behavior of the lateral sensor characterized by Cannara *et al* [15] could be corrected using the procedure outlined herein.

Acknowledgments

Appendix. Implementation

We present two subroutines (in the MATLAB language) that may be implemented in the AFM data processing software to automate the protocol proposed herein.

Steps (iii) and (iv) of the protocol are performed by running the subroutine `calibrate` on the data acquired in step (ii). The input parameters are the photodiode voltage signal V_{PD} (Vpd) and the Z-piezo displacement Z_p (Zp). The routine returns V_{PD}^* (Vpds), $a_1 = S_{PD}^{-1}(V_{PD}^*)$ (a1) and a_3 (a3).

```
function [Vpds, a1, a3] = calibrate(Vpd, Zp)
% Fit Zp = b3*Vpd^3 + b2*Vpd^2 + b1*Vpd + b0
P = polyfit(Vpd, Zp, 3);
b3 = P(1); b2 = P(2); b1 = P(3); b0 = P(4);
% Calculate Vpds, the inflection point
Vpds = -b2/(3*b3);
% Shift the center of the polynomial to Vpds
a3 = b3;
a1 = b1 + 2*b2*Vpds + 3*b3*Vpds^2;
```

Step (ix) of the protocol is performed by running `apply_calibration` on the data acquired in step (viii). The input parameters are the voltage signal V_{PD} (Vpd), the resting signal V_{PD}^0 (Vpd0) and the calibration parameters Vpds, a1 and a3, calculated by `calibrate`. If the conventional (linear) analysis is required, just provide zero for both a3 and Vpds.

```
function Zc = apply_calibration
                   (Vpd, Vpd0, Vpds, a1, a3)
% Calculate a0 such that Zc(Vpd0) = 0
a0 = -a3*(Vpd0 - Vpds)^3 - a1*(Vpd0 - Vpds);
% Apply the calibration
Zc = a3*(Vpd - Vpds).^3 + a1*(Vpd - Vpds) + a0;
```

References

[1] Binnig G, Quate C F and Gerber C 1986 Atomic force microscope *Phys. Rev. Lett.* **56** 930–3

[2] Cappella B and Dietler G 1999 Force–distance curves by atomic force microscopy *Surf. Sci. Rep.* **34** 1–104

[3] Butt H J, Cappella B and Kappl M 2005 Force measurements with the atomic force microscope: technique, interpretation and applications *Surf. Sci. Rep.* **59** 1–152

[4] Meyer G 1988 Novel optical approach to atomic force microscopy *Appl. Phys. Lett.* **53** 2400–2

[5] Schaffer T E and Hansma P K 1998 Characterization and optimization of the detection sensitivity of an atomic force microscope for small cantilevers *J. Appl. Phys.* **84** 4661–6

[6] Beaulieu L Y, Godin M, Laroche O, Tabard-Cossa V and Grutter P 2006 Calibrating laser beam deflection systems for use in atomic force microscopes and cantilever sensors *Appl. Phys. Lett.* **88** 083108

[7] Butt H J 1994 A technique for measuring the force between a colloidal particle in water and a bubble *J. Colloid Interface Sci.* **166** 109–17

[8] Pierce M, Stuart J, Pungor A, Dryden P and Hlady V 1994 Adhesion force measurements using an atomic-force microscope upgraded with a linear position-sensitive detector *Langmuir* **10** 3217–21

[9] Schaffer T E 2002 Force spectroscopy with a large dynamic range using small cantilevers and an array detector *J. Appl. Phys.* **91** 4739–46

[10] Olympus Corporation 2006 *Micro Cantilever OMCL Series Catalog* Tokyo (URL http://www.olympus.co.jp/probe/)

[11] Hutter J L and Bechhoefer J 1993 Calibration of atomic-force microscope tips *Rev. Sci. Instrum.* **64** 1868–73

[12] Butt H J and Jaschke M 1995 Calculation of thermal noise in atomic-force microscopy *Nanotechnology* **6** 1–7

[13] Burnham N A, Chen X, Hodges C S, Matei G A, Thoreson E J, Roberts C J, Davies M C and Tendler S J B 2003 Comparison of calibration methods for atomic-force microscopy cantilevers *Nanotechnology* **14** 1–6

[14] Asay D B and Kim S H 2006 Direct force balance method for atomic force microscopy lateral force calibration *Rev. Sci. Instrum.* **77** 043903

[15] Cannara R J, Eglin M and Carpick R W 2006 Lateral force calibration in atomic force microscopy: a new lateral force calibration method and general guidelines for optimization *Rev. Sci. Instrum.* **77** 053701